- A *scaling approach*, which starts with the interacting but isolated atom ($V(k) = 0$), and considers the effect of immersing it in an electron sea, gradually integrating out lower and lower-energy electrons.

The adiabatic approach involves "dialing up" the interaction, as shown by the horizontal arrow in Figure 16.11. From the adiabatic perspective, the ground state remains in a Fermi liquid. In principle, one might imagine the possibiity of a phase transition at some finite interaction strength U, but in a single-impurity model, with a finite number of local degrees of freedom, we don't expect any symmetry-breaking phase transitions. In the scaling approach, we follow the physics as a function of ever-decreasing energy scale, loosely equivalent to "dialing down" the temperature, as shown by the vertical arrow in Figure 16.11. The scaling approach starts from an atomic perspective: it allows us to understand the formation of local moments and, at lower temperatures, how a Fermi liquid can develop through the interaction of an isolated magnetic moment with an electron sea.

We shall first discuss one of the most basic manifestations of the Kondo effect: the appearance of a Kondo resonance in the spectral function of the localized electron. This part of our analysis will involve rather qualitative reasoning based on the ideas of adiabaticity introduced in earlier chapters. Afterwards we adopt the scaling approach, deriving the Kondo model and describing low-energy coupling between the local moments and conduction electrons by using a *Schrieffer–Wolff transformation* of the Anderson model. Finally, we discuss the concept of renormalization and apply it to the Kondo model, following the evolution of the physics from the local moment to the Fermi liquid.

16.6.1 Adiabaticity and the Kondo resonance

The adiabatic approach allows us to qualitatively understand the emergence of a remarkable resonance in the excitation spectrum of the localized f-electron, the *Kondo resonance*. This resonance is simply the adiabatic renormalization of the Friedel–Anderson resonance seen in the non-interacting Anderson model. Its existence was first inferred by Abrikosov and Suhl [44, 45], and the term *Abrikosov–Suhl resonance* is the historically correct name for the resonance.

To understand the Kondo resonance, we shall study the effects of interactions on the f-spectral function

$$A_f(\omega) = \frac{1}{\pi}\mathrm{Im}\, G_f(\omega + i\eta), \tag{16.73}$$

where $G_f(\omega - i\delta) =$ is the advanced f-Green's function. From a spectral decomposition (Section 9.7.1), we know that

$$A_f(\omega) = \begin{cases} \overbrace{\sum_\lambda \left|\langle\lambda|f_\sigma^\dagger|\phi_0\rangle\right|^2 \delta(\omega - [E_\lambda - E_0])}^{\text{energy distribution for adding one } f\text{-electron}} & (\omega > 0) \\ \underbrace{\sum_\lambda |\langle\lambda|f_\sigma|\phi_0\rangle|^2 \delta(\omega - [E_0 - E_\lambda])}_{\text{energy distribution for removing one } f\text{-electron}} & (\omega < 0), \end{cases} \tag{16.74}$$

where E_λ and E_0 are the excited and ground-state energies, respectively. For negative energies, $\omega < 0$, this spectrum corresponds to the energy spectrum of electrons emitted in X-ray photoemission, while for positive energies, $\omega > 0$, the spectral function can be measured from inverse X-ray photoemission [46, 47]. The weight beneath the Fermi energy determines the f-charge of the ion:

$$\langle n_f \rangle = 2 \int_{-\infty}^{0} d\omega A_f(\omega). \tag{16.75}$$

In a magnetic ion such as a cerium atom in a $4f^1$ state, this quantity is just a little below unity.

Figure (16.12.) illustrates the effect of the interaction on the f-spectral function. In the non-interacting limit ($U = 0$), the f-spectral function is a Lorentzian of width Δ. If we turn on the interaction U, being careful to shift the f-level position beneath the Fermi energy to maintain a constant occupancy, the resonance splits into three peaks: two at energies $\omega = E_f$ and $\omega = E_f + U$ corresponding to the energies for a valence fluctuation, plus an additional central Kondo resonance associated with the spin fluctuations of the local moment.

When the interaction is much larger than the hybridization width, $U >> \Delta$, one might expect no spectral weight left at low energies. But it turns out that the spectral

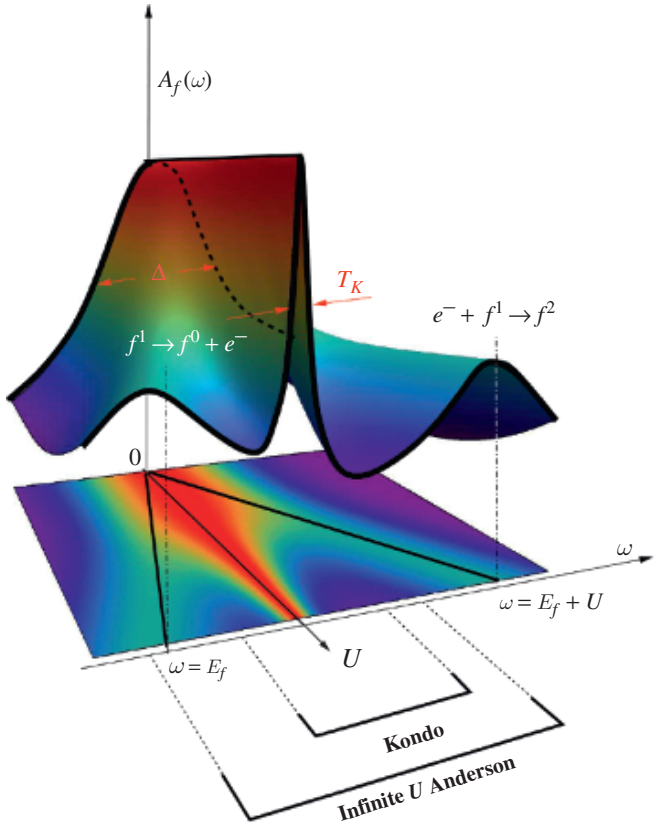

Schematic illustration of the formation of a Kondo resonance in the f-spectral function $A_f(\omega)$ as interaction strength U is turned on. Here, the interaction is turned on while maintaining a constant f-occupancy, by shifting the bare f-level position beneath the Fermi energy. The lower part of diagram is the density plot of the f-spectral function, showing how the non-interacting resonance at $U = 0$ splits into upper and lower atomic peaks at $\omega = E_f$ and $\omega = E_f + U$. **Fig. 16.12**

function at the Fermi energy is an adiabatic invariant determined by the scattering phase shift δ_f:

$$A_f(\omega = 0) = \frac{\sin^2 \delta_f}{\pi \Delta}. \tag{16.76}$$

This result, due to Langreth [48, 49], guarantees that a Kondo resonance is always present at the Fermi energy. Now the total spectral weight $\int_{-\infty}^{\infty} d\omega A_f(\omega) = 1$ is conserved, so if $|E_f|$ and U are both large compared with Δ, most of this weight will be lie far from the Fermi energy, leaving a small residue $Z << 1$ in the Kondo resonance. If the area under the Kondo resonance is Z, since the height of Kondo resonance is fixed at $\sim 1/\Delta$, the renormalized hybridization width Δ^* must be of order $Z\Delta$. This scale is set by the Kondo temperature, so that $Z\Delta \sim T_K$.

The Langreth relation (16.76) follows from the analytic form of the f-Green's function near the Fermi energy. For a single magnetic ion, we expect that the interactions between electrons can be increased continuously without any risk of instabilities, so that the excitations of the strongly interacting case remain in one-to-one correspondence with the excitations of the non-interacting case $U = 0$, forming a *local Fermi liquid*. In this local Fermi liquid, the interactions give rise to an f-electron self-energy, which at zero temperature takes the form

$$\Sigma_I(\omega - i\eta) = \Sigma_I(0) + (1 - Z^{-1})\omega + iA\omega^2, \tag{16.77}$$

at low energies. As discussed in Chapter 7, the quadratic energy dependence of $\Sigma_I(\omega) \sim \omega^2$ follows from the Pauli exclusion principle, which forces a quadratic energy dependence of the phase space for the emission of a particle–hole pair. The *wavefunction renormalization* Z, representing the overlap with the state containing one additional f-quasiparticle, is less than unity, $Z < 1$. Using the result (16.77), the low-energy form of the f-electron propagator is

$$\begin{aligned} G_f^{-1}(\omega - i\eta) &= \omega - E_f - i\Delta - \Sigma_I(\omega) = Z^{-1}\big[\omega - \overbrace{Z(E_f + \Sigma_I(0))}^{E_f^*} - i\overbrace{Z\Delta}^{\Delta^*} - iO(\omega^2)\big] \\ G_f(\omega - i\eta) &= \frac{Z}{\omega - E_f^* - i\Delta^* - iO(\omega^2)}. \end{aligned} \tag{16.78}$$

This corresponds to a renormalized resonance of reduced weight $Z < 1$, located at postion E_f^* with renormalized width $\Delta^* = Z\Delta$. Now by (16.32) and (16.34), the f-Green's function determines the t-matrix of the conduction electrons, $t(\omega + i\eta) = V^2 G_f(\omega + i\eta) = -(\pi\rho)^{-1} e^{i\delta(\omega)} \sin\delta(\omega)$, so the phase of the f-Green's function at the Fermi energy determines the scattering phase shift δ_f, hence $G_f(0 + i\eta) = (G_f(0 - i\eta))^* = -|G_f(0)|e^{i\delta_f}$. This implies that the scattering phase shift at the Fermi energy is

$$\delta_f = \mathrm{Im}\left(\ln[-G_f^{-1}(\omega - i\eta)]\right)\Big|_{\omega=0} = \tan^{-1}\left(\frac{\Delta^*}{E_f^*}\right). \tag{16.79}$$

Eliminating $E_f^* = \Delta^* \cot\delta_f$ from (16.78), we obtain

$$G_f(0 + i\eta) = -\frac{Z}{\Delta^*} e^{-i\delta_f} \sin\delta_f = -\frac{1}{\Delta} e^{-i\delta_f} \sin\delta_f, \tag{16.80}$$

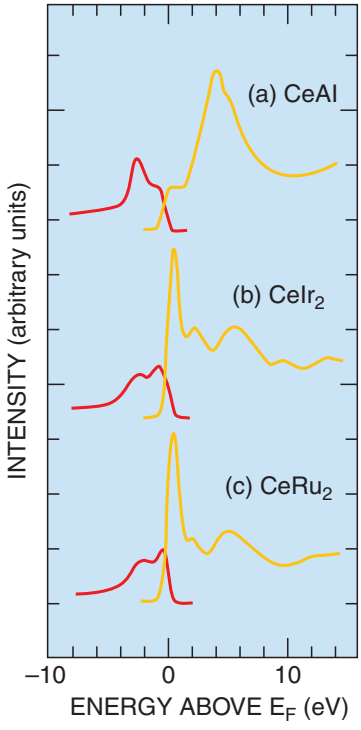

Fig. 16.13 Spectral functions for three different cerium f-electron materials, measured using X-ray photoemission (below the Fermi energy) and inverse X-ray photoemission (above the Fermi energy). CeAl is an antiferromagnet and does not display a Kondo resonance. Reprinted with permission from J. W. Allen, *et al., Phys. Rev.*, vol. 28, p. 5347, 1983. Copyright 1983 by the American Physical Society.

so that

$$A_f(0) = \frac{1}{\pi}\mathrm{Im}\, G_f(0 - i\eta) = \frac{\sin^2 \delta_f}{\pi \Delta} \tag{16.81}$$

is an adiabatic invariant.

Photoemission studies do reveal the three-peaked structure characteristic of the Anderson model in many Ce systems, such as $CeIr_2$ and $CeRu_2$ [47] (see Figure 16.13). Materials in which the Kondo resonance is wide enough to be resolved are the more mixed-valent materials in which the f-valence departs significantly from unity. Three-peaked structures have also been observed in certain U $5f$ materials such as UPt_3 and UAl_2 materials [50], but it has not yet been resolved in UBe_{13}. A three-peaked structure has recently been observed in $4f$ Yb materials, such as $YbPd_3$, where the $4f^{13}$ configuration contains a single f-hole, so that the positions of the three peaks are reversed relative to Ce [51].

16.7 Renormalization concept

The Anderson model illustrates a central theme of condensed matter physics: the existence of physics on several widely spaced energy scales. In particular, the scale at which local

moments form in f-electron systems is of the order of the Coulomb energy U, a scale of order 10eV, while the Kondo effect occurs at a scale a thousand times smaller, of order 10K$\sim$ 1 meV. When energy scales are well separated like this, we use the *renormalization group* to fold the key effects of the high-energy physics into a small set of parameters that control the low-energy physics [12, 16, 17, 31].

Renormalization is built on the idea that the low-energy physics of a system only depends on certain gross features of the high-energy physics. The family of systems with the same low-energy excitation spectrum constitute a *universality class* of models (Figure 16.14). We need the concept of universality, for without it we would be lost: we could not hope to capture the physics of real-world systems with our simplified Hamiltonian models. The Anderson model is itself a renormalized Hamiltonian, notionally derived from the elimination of high-energy excitations from "the" microscopic Hamiltonian.

To carry out renormalization, the Hamiltonian of interest $H(D)$ is parameterized by its cut-off energy scale D, the energy of the largest excitations. Renormalization involves reducing the cut-off to a slightly smaller value, $D \to D' = D/b$, where $b > 1$. The excitations in the energy window $E \in [D', D]$ that are removed by this process are said

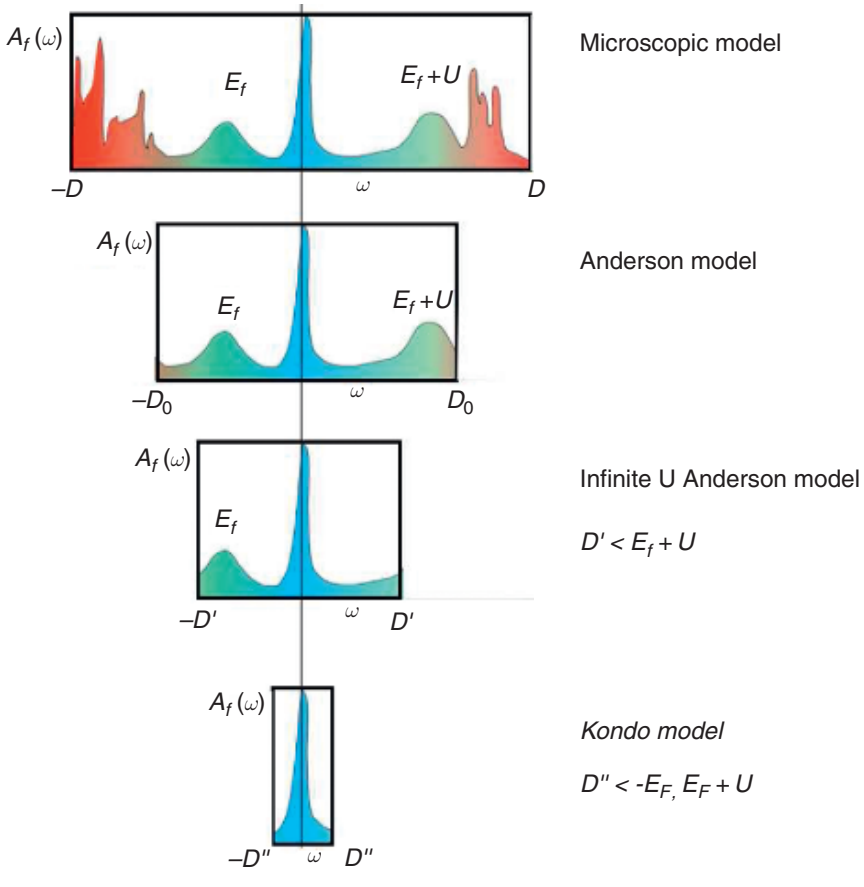

Fig. 16.14 Scaling concept. Low-energy model Hamiltonians are obtained from the detailed original model by integrating out the high-energy degrees of freedom. At each stage, the physics described by the model spans a successively lower frequency window in the excitation spectrum.

to have been integrated out of the Hilbert space, and in so doing they give rise to a new *effective Hamiltonian* $\tilde{H}_L$ that continues to faithfully describe the remaining low-energy degrees of freedom. The energy scales are then rescaled to obtain a new $H(D') = b\tilde{H}_L$, and the whole process is repeated.

Generically, the Hamiltonian can be divided into a block-diagonal form:

$$H = \left[\begin{array}{c|c} H_L & V^\dagger \\ \hline V & H_H \end{array}\right], \tag{16.82}$$

where H_L and H_H act on states in the low-energy and high-energy subspaces, respectively, and V and $V^\dagger$ provide the matrix elements between them. The high-energy degrees of freedom may be integrated out[4] by carrying out a canonical transformation that eliminates the off-diagonal elements in this Hamiltonian $\tilde{H}_L$:

$$H(D) \to \tilde{H} = UH(D)U^\dagger = \left[\begin{array}{c|c} \tilde{H}_L & 0 \\ \hline 0 & \tilde{H}_H \end{array}\right]. \tag{16.83}$$

One then projects out the low-energy component of the block-diagonalized Hamiltonian $\tilde{H}_L = P\tilde{H}P$. Finally, by rescaling

$$H(D') = b\tilde{H}_L \tag{16.84}$$

one arrives at a new Hamiltonian describing the physics on the reduced scale. The transformation from $H(D)$ to $H(D')$ is referred to as a renormalization group (RG) transformation. This term was coined long ago, although the transformation does not form a real group, since there is no inverse transformation.

Repeated application of the RG procedure leads to a family of Hamiltonians $H(D)$ (see Figure 16.14). By taking the limit $b \to 1$, these Hamiltonians evolve, or "flow" continuously with D. Typically, H will contain a series of dimensionless parameters (coupling constants) $\{g_i\}$ which denote the strength of various interaction terms in the Hamiltonian. The evolution of these parameters with cut-off is given by a scaling equation. In the simplest case,

$$\frac{\partial g_j}{\partial \ln D} = \beta_j(\{g_i\}).$$

A negative β function denotes a "*relevant*" parameter which grows as the cut-off is reduced. A positive β function denotes an "*irrelevant*" parameter which shrinks towards zero as the cut-off is reduced. There are two types of event that can occur in such a scaling procedure:

- Crossover. When the cut-off energy scale D passes the characteristic energy scale of a particular class of high-frequency excitations, then at lower energies these excitations may only occur via a virtual process. When the effects of the virtual fluctuations associated with these high-energy process are included in the Hamiltonian, it changes its structure.

[4] The term "integrating out" is originally derived from the path integral formulation of the renormalization group, in which high-energy degrees of freedom are removed by integrating over these variables inside the path integral.

- Fixed point. If the cut-off energy scale drops below the lowest energy scale in the problem, then there are no further changes to occur in the Hamiltonian, which will now remain invariant under the scaling procedure (so that the β function of all remaining parameters in the Hamiltonian must vanish). This fixed-point Hamiltonian describes the essence of the low-energy physics.

Local-moment physics involves a sequence of such cross-overs (Figure 16.14.). The highest energy scales in the Anderson model are associated with valence fluctuations into the empty and doubly occupied states:

$$\begin{aligned} f^1 &\leftrightharpoons f^2 \qquad \Delta E_I = U + E_f > 0 \\ f^1 &\leftrightharpoons f^0 \qquad \Delta E_{II} = -E_f > 0. \end{aligned} \tag{16.85}$$

The successive elimination of these processes leads to two cross-overs. Suppose ΔE_I is the largest scale; then, once $D < \Delta E_I$, charge fluctuations into the doubly occupied state are eliminated and the remaining low-energy Hilbert space of the atom is

$$D < E_f + U: \qquad |f^0\rangle, \qquad |f^1, \sigma\rangle \qquad \left(\sigma = \pm\frac{1}{2}\right). \tag{16.86}$$

The operators that span this space are called *Hubbard operators* [52], and they are denoted as follows:

$$\begin{aligned} X_{\sigma 0} &= |f^1, \sigma\rangle\langle f^0| = P f_\sigma^\dagger, \qquad & X_{0\sigma} &= |f^0\rangle\langle f^1, \sigma| = f_\sigma^\dagger P, \\ X_{\sigma\sigma'} &= |f^1, \sigma\rangle\langle f^1, \sigma'|, \end{aligned} \tag{16.87}$$

where $P = (1 - n_{f\uparrow} n_{f\downarrow})$ projects out doubly occupied states. (Note that the Hubbard operators $X_{\sigma 0} = P f_\sigma^\dagger$ cannot be treated as simple creation operators, for they do not satisfy the canonical anticommutation algebra.) The corresponding renormalized Hamiltonian is the *Infinite U Anderson model*.

$$H = \sum_{\mathbf{k},\sigma} \epsilon_{\mathbf{k}} n_{\mathbf{k}\sigma} + \left[V(\mathbf{k}) c_{\mathbf{k}\sigma}^\dagger X_{0\sigma} + V(\mathbf{k})^* X_{\sigma 0} c_{\mathbf{k}\sigma} \right] + E_f \sum_\sigma X_{\sigma\sigma}. \tag{16.88}$$

Infinite U Anderson model

In this model, all the interactions are hidden inside the Hubbard operators.

Finally, once $D < \Delta E_{II}$, the low-energy Hilbert space no longer involves the f^2 *or* f^0 states. The object left behind is a *quantum top* – a quantum mechanical object with purely spin degrees of freedom and a two-dimensional[5] Hilbert space:

$$|f^1, \sigma\rangle \qquad \left(\sigma = \pm\frac{1}{2}\right).$$

[5] In the simplest version of the Anderson model, the local moment is $S = \frac{1}{2}$, but in more realistic atoms much larger moments can be produced. For example, an electron in a Ce^{3+} ion atom lives in a $4f^1$ state. Here spin–orbit coupling combines orbital and spin angular momentum into a total angular moment $j = l - \frac{1}{2} = \frac{5}{2}$. The cerium ion that forms thus has a spin $j = \frac{5}{2}$ with a spin degeneracy of $2j + 1 = 6$. In multi-electron atoms, the situation can become still more complex, involving Hund's coupling between atoms.

Now the residual spin degrees of freedom still interact with the surrounding conduction sea, for virtual charge fluctuations, in which an electron temporarily migrates off of or onto the ion, lead to spin exchange between the local moment and the conduction sea. There are two such virtual processes:

$$\begin{array}{lll} e_\uparrow + f^1_\downarrow & \leftrightarrow f^2 \leftrightarrow e_\downarrow + f^1_\uparrow & \Delta E_I \sim U + E_f \\ e_\uparrow + f^1_\downarrow & \leftrightarrow e_\uparrow + e_\downarrow \leftrightarrow e_\downarrow + f^1_\uparrow & \Delta E_{II} \sim -E_f . \end{array} \tag{16.89}$$

In both cases, spin exchange only takes place in the singlet channel, $S = 0$, state. From second-order perturbation theory, we know that these virtual charge fluctuations will selectively lower the energy of the singlet configurations by an amount of order $\Delta E = -J$, where

$$J \sim V^2 \left[\frac{1}{\Delta E_1} + \frac{1}{\Delta E_2} \right] = V^2 \left[\frac{1}{-E_f} + \frac{1}{E_f + U} \right]. \tag{16.90}$$

Here V is the size of the hybridization matrix element near the Fermi surface. The selective reduction in the energy of the singlet channel constitutes an effective antiferromagnetic interaction between the conduction electrons and the local moment. If we introduce $\vec{\sigma}(0) = \sum_{k,k'} c^\dagger_{k\alpha} \vec{\sigma}_{\alpha\beta} c_{k'\beta}$, measuring the electron spin at the origin, then the effective interaction that lowers the energy of singlet combinations of conduction and f-electrons will have the form $H_{eff} \sim J\vec{\sigma}(0) \cdot \vec{S}_f$. The resulting low-energy Hamiltonian that describes the interaction of a spin with a conduction sea is the deceptively simple Kondo model:

$$H = \sum_{k\sigma} \epsilon_k c^\dagger_{k\sigma} c_{k\sigma} + \overbrace{J \psi^\dagger(0) \vec{\sigma}\, \psi(0) \cdot \vec{S}_f}^{\Delta H} . \tag{16.91}$$

Kondo model

This heuristic argument was ventured in 1961 in Anderson's paper [7] on local moment formation. At the time, the antiferromagnetic sign in this interaction was entirely unexpected, for it had long been assumed that exchange forces always induce a ferromagnetic interaction between the conduction sea and local moments. The innocuous-looking sign difference has deep consequences for the physics of local moments at low temperatures, giving rise to an interaction that grows as the temperature is lowered, ultimately leading to a final crossover into a low-energy Fermi liquid fixed point. The remaining sections of this chapter are devoted to following this process in detail.

16.8 Schrieffer–Wolff transformation

We now carry out the transformation that links the Anderson and Kondo models via a canonical transformation, first introduced by Schrieffer and Wolff [10, 11]. This transformation is a kind of one-step renormalization process in which the valence fluctuations are integrated out of the Anderson model. When a local moment forms, hybridization with

the conduction sea induces virtual charge fluctuations. It's useful to consider dividing the Hamiltonian into two terms,

$$H = H_1 + \lambda \mathcal{V},$$

where λ is an expansion parameter. Here,

$$H_1 = H_{band} + H_{atomic} = \left[\begin{array}{c|c} H_L & 0 \\ \hline 0 & H_H \end{array}\right]$$

is diagonal in the low-energy f^1 (H_L) and the high-energy f^2 or f^0 (H_H) subspaces, whereas the hybridization term

$$\mathcal{V} = H_{mix} = \sum_{\mathbf{k}\sigma} \left[V_{\vec{k}} c^\dagger_{k\sigma} f_\sigma + \text{H.c.}\right] = \left[\begin{array}{c|c} 0 & V^\dagger \\ \hline V & 0 \end{array}\right]$$

provides the off-diagonal matrix elements between these two subspaces. The idea of the Schrieffer–Wolff transformation is to carry out a canonical transformation that returns the Hamiltonian to block-diagonal form:

$$\mathcal{U}\left[\begin{array}{c|c} H_L & \lambda V^\dagger \\ \hline \lambda V & H_H \end{array}\right]\mathcal{U}^\dagger = \left[\begin{array}{c|c} H^* & 0 \\ \hline 0 & H' \end{array}\right]. \tag{16.92}$$

This is a *renormalized* Hamiltonian, and the block-diagonal part of this matrix, $H^* = P_L H' P_L$, in the low-energy subspace provides an *effective* Hamiltonian for the low-energy physics. We now set $\mathcal{U} = e^S$, referring to S as the *action operator*. Now since $\mathcal{U}^\dagger = \mathcal{U}^{-1} = e^{-S}$, this implies that the action operator $S^\dagger = -S$ is anti-Hermitian. Writing S as a power series in λ,

$$S = \lambda S_1 + \lambda^2 S_2 + \cdots,$$

and using the identity $e^A B e^{-A} = B + [A, B] + \frac{1}{2!}[A, [A, B]] + \cdots$, (16.92) can be expanded in powers of λ as follows:

$$e^S(H_1 + \lambda\mathcal{V})e^{-S} = H_1 + \lambda\Big(\mathcal{V} + [S_1, H_1]\Big) + \lambda^2\left(\frac{1}{2}[S_1, [S_1, H]] + [S_1, \mathcal{V}] + [S_2, H_1]\right) + \cdots.$$

Since $\mathcal{V}$ is not diagonal, by requiring

$$[S_1, H_1] = -\mathcal{V}, \tag{16.93}$$

we can eliminate all off-diagonal components to leading order in λ. To second order,

$$e^S(H_1 + \lambda\mathcal{V})e^{-S} = H_1 + \lambda^2\left(\frac{1}{2}[S_1, \mathcal{V}] + [S_2, H_1]\right) + \cdots. \tag{16.94}$$

Since $[S_1, \mathcal{V}]$ is block-diagonal, we can satisfy (16.92) to second order by requiring $S_2 = 0$, so that, to this order, the renormalized Hamiltonian has the form

$$H^* = H_L + \lambda^2 \Delta H, \tag{16.95}$$

where

$$\Delta H = \frac{1}{2} P_L [S_1, \mathcal{V}] P_L + \cdots \tag{16.96}$$

is an interaction term induced by virtual fluctuations into the high-energy manifold. Writing the action operator in matrix form,

$$S = \left[\begin{array}{c|c} 0 & -s^\dagger \\ \hline s & 0 \end{array}\right], \tag{16.97}$$

and substituting into (16.93), we obtain $V = -sH_L + H_H s$. Now since $(H_L)_{ab} = E_a^L \delta_{ab}$ and $(H_H)_{ab} = E_a^H \delta_{ab}$ are diagonal, it follows that

$$s_{ab} = \frac{V_{ab}}{E_a^H - E_b^L}, \qquad -s_{ab}^\dagger = \frac{V_{ab}^\dagger}{E_a^L - E_b^H}, \tag{16.98}$$

or, more schematically,

$$S = \sum_{H,L} \left(|H\rangle \frac{\langle H|V|L\rangle}{E_H - E_L} \langle L| - \text{H.c.} \right) + O(V^3). \tag{16.99}$$

From (16.98) we obtain

$$\Delta H_{LL'} = -\frac{1}{2}(V^\dagger s + s^\dagger V)_{LL'} = -\frac{1}{2}\sum_H (V_{LH}^\dagger V_{HL'}) \left[\frac{1}{E_H - E_L} + \frac{1}{E_H - E_{L'}} \right]. \tag{16.100}$$

Some important points about this result:

- We recognize (16.100) as a simple generalization of second-order perturbation theory, including off-diagonal matrix elements by averaging over initial- and final-state energy denominators.
- ΔH can also be written

$$\Delta H_{LL'} = \frac{1}{2}[T(E_L) + T(E_{L'})],$$

where

$$\hat{T}(E) = P_L \mathcal{V} \frac{P_H}{E - H_1} \mathcal{V} P_L$$
$$T_{LL'}(E) = \sum_{|H\rangle} \left[\frac{V_{LH}^\dagger V_{HL'}}{E - E_H} \right] \tag{16.101}$$

is the leading-order expression for the many-body scattering t-matrix induced by scattering off $\mathcal{V}$. We can thus relate ΔH to a scattering amplitude, and schematically represent it by a Feynman diagram, illustrated in Figure 16.15.

- If the separation of the low- and high-energy subspaces is large, we can take $E_L \sim E_{L'}$, so that

$$\Delta H = T(E_L) = -\frac{1}{\Delta E_{HL}} (\mathcal{V} P_H \mathcal{V}), \tag{16.102}$$

where $\Delta E_{HL} = E_H - E_L$ is the energy of excitation into the high-energy subspace and $P_H = \sum_{|H\rangle} |H\rangle\langle H|$.

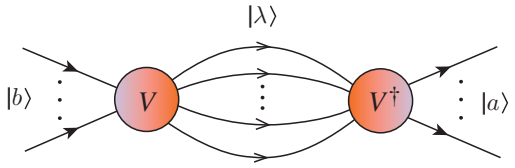

Fig. 16.15 A t-matrix representation of the interaction induced between states $|b\rangle$ and $|a\rangle$ by integrating out the virtual fluctuations into the high-energy states $|\lambda\rangle$.

We now apply this method to the Anderson model for which the atomic ground state is a local-moment f^1 configuration. In this case, there are two high-energy intermediate states, corresponding to f^0 and f^2 configurations. When a conduction electron or hole is excited into the localized f-state to create these excited-state configurations, the corresponding excitation energies are $\Delta E(f^1 \to f^0) = -E_f$ and $\Delta E(f^1 \to f^2) = E_f + U$. The hybridization $\mathcal{V} = \sum_{\mathbf{k}\sigma}\left[V(\mathbf{k})c^\dagger_{\mathbf{k}\sigma}f_\sigma + \text{H.c.}\right]$ generates virtual fluctuations into these excited states. Using (16.102), the interaction induced by these fluctuations is given by

$$\begin{aligned}\Delta H &= -\frac{VP[f^2]V}{E_f+U} - \frac{VP[f^0]V}{-E_f} \\ &= -\sum_{k\alpha,k'\beta} V^*_{k'}V_k\left[\frac{\overbrace{(c^\dagger_{k\alpha}f_\alpha)(f^\dagger_\beta c_{k'\beta})}^{f^1+e^-\leftrightarrow f^2}}{E_f+U} + \frac{\overbrace{(f^\dagger_\beta c_{k'\beta})(c^\dagger_{k\alpha}f_\alpha)}^{f^1\leftrightarrow f^0+e^-}}{-E_f}\right]P_{n_f=1},\end{aligned} \tag{16.103}$$

where $P_{n_f=1} = (n_{f\uparrow} - n_{f\downarrow})^2$ projects into the subspace of unit occupancy. Using the Fierz identity[6] $2\delta_{\alpha\gamma}\delta_{\eta\beta} = \delta_{\alpha\beta}\delta_{\eta\gamma} + \vec{\sigma}_{\alpha\beta}\cdot\vec{\sigma}_{\eta\gamma}$, we may recast the spin exchange terms in terms of Pauli matrices, as follows:

$$\begin{aligned}(c^\dagger_{k\alpha}f_\alpha)(f^\dagger_\beta c_{k'\beta}) &= (c^\dagger_{k\alpha}f_\gamma)(f^\dagger_\eta c_{k'\beta}) \times \overbrace{(\delta_{\alpha\gamma}\delta_{\eta\beta})}^{\frac{1}{2}(\delta_{\alpha\beta}\delta_{\eta\gamma}+\vec{\sigma}_{\alpha\beta}\cdot\vec{\sigma}_{\eta\gamma})} \\ &= \frac{1}{2}c^\dagger_{k\alpha}c_{k'\alpha} - (c^\dagger_{k\alpha}\vec{\sigma}_{\alpha\beta}c_{k'\beta})\cdot\vec{S}_f,\end{aligned} \tag{16.104}$$

and similarly

$$(f^\dagger_\beta c_{k'\beta})(c^\dagger_{k\alpha}f_\alpha) = -\frac{1}{2}c^\dagger_{k\alpha}c_{k'\alpha} - (c^\dagger_{k\alpha}\vec{\sigma}_{\alpha\beta}c_{k'\beta})\cdot\vec{S}_f \tag{16.105}$$

(where we have replaced $n_f = 1$ and dropped residual constants in both cases). The operator

$$\vec{S}_f \equiv f^\dagger_\sigma\left(\frac{\vec{\sigma}_{\alpha\beta}}{2}\right)f_\beta, \qquad (n_f = 1) \tag{16.106}$$

describes the spin of the f-electron. The induced interaction is then

$$\Delta H = \sum_{k\alpha,k'\beta} J_{k,k'}c^\dagger_{k\alpha}\vec{\sigma}_{\alpha\beta}c_{k'\beta}\cdot\vec{S}_f + H', \tag{16.107}$$

[6] This identity is obtained by expanding an arbitrary two-dimensional matrix A in terms of Pauli matrices. If we write $A_{\alpha\beta} = \frac{1}{2}\text{Tr}[A\underline{1}]\delta_{\alpha\beta} + \frac{1}{2}\text{Tr}[A\vec{\sigma}]\cdot\vec{\sigma}_{\alpha\beta}$ and read off the coefficients of A inside the traces, we obtain the inequality.

where

$$J_{k,k'} = V_{k'}^* V_k \left[\overbrace{\frac{1}{E_f + U}}^{f^1 + e^- \leftrightarrow f^2} + \overbrace{\frac{1}{-E_f}}^{f^1 \leftrightarrow f^0 + e^-} \right] \tag{16.108}$$

is the Kondo coupling constant.

Notice how, in the low-energy subspace, the occupancy of the f-state is constrained to $n_f = 1$. This fermionic representation (16.106) of the spin operator proves to be very useful. Apart from a constant, the second term,

$$H' = -\frac{1}{2} \sum_{k,k'\sigma} V_{k'}^* V_k \left[\frac{1}{E_f + U} + \frac{1}{E_f} \right] c_{k\sigma}^\dagger c_{k'\sigma},$$

is a residual potential scattering term. This term vanishes for the particle–hole symmetric case $E_f = -(E_f + U)$, and will be dropped since it does not involve the internal dynamics of the local moment. Summarizing, the effect of the high-frequency valence fluctuations is to induce an antiferromagnetic coupling between the local spin density of the conduction electrons and the local moment:

$$H = \sum_{k\sigma} \epsilon_k c_{k\sigma}^\dagger c_{k\sigma} + \sum_{k,k'} J_{k,k'} c_{k\alpha}^\dagger \vec{\sigma} c_{k'\beta} \cdot \vec{S}_f. \tag{16.109}$$

This is the famous Kondo model. For many purposes, the k-dependence of the coupling constant can be dropped, so that the model takes the simpler form shown in (16.91):

$$H = \sum_{k\sigma} \epsilon_k c_{k\sigma}^\dagger c_{k\sigma} + \overbrace{J \vec{\sigma}(0) \cdot \vec{S}_f}^{\Delta H}, \tag{16.110}$$

Kondo model

where $\psi_\alpha(0) = \sum_k c_{k\alpha}$ is the electron operator at the origin and $\vec{\sigma}(0) = \psi^\dagger(0) \vec{\sigma} \psi(0)$ is the spin density at the origin. In other words, there is a simple point interaction between the spin density of the metal at the origin and the local moment.

Example 16.4 Details of the Schrieffer–Wolff transformation.
Show that the action operator S for the canonical transformation $H \to H^* = e^S H e^{-S}$ that effects the Schrieffer–Wolff transformation from the Anderson model (16.5) to the Kondo model (16.110) is given by [10, 11]

$$S = \sum_{\mathbf{k},\sigma} \left[V_{\mathbf{k}} c_{\mathbf{k}\sigma}^\dagger f_\sigma \left(\frac{1 - n_{f\,-\sigma}}{\epsilon_{\mathbf{k}} - E_f} + \frac{n_{f\sigma}}{\epsilon_{\mathbf{k}} - (E_f + U)} \right) - \text{H.c.} \right] + O(V^3). \tag{16.111}$$

Solution

Using (16.98), we may write the action operator S as

$$S = \sum_{H,L} \left[|H\rangle \frac{\langle H|V|L\rangle}{E_H - E_L} \langle L| - \text{H.c.} \right] + O(V^3), \tag{16.112}$$

where, L and H denote the low- and high-energy subspaces, respectively. For the Anderson model, $\hat{V} = \sum_{\mathbf{k},\sigma} (V_{\mathbf{k}} c^\dagger_{\mathbf{k}\sigma} f_\sigma + \text{H.c.})$ is the hybridization, while the low-energy Hilbert space is the states with $n_f = 1$. The projector into the low-energy subspace H is $P_L = (n_{f\uparrow} - n_{f\downarrow})^2$, so we may write $\langle H|V|L\rangle = \langle H|VP_L|L\rangle$, so that

$$S = \sum_{H,L,\,\mathbf{k}\sigma} \left(|H\rangle\langle H| \frac{(V_{\mathbf{k}} c^\dagger_{\mathbf{k}\sigma} f_\sigma + V^*_{\mathbf{k}} f^\dagger_\sigma c_{\mathbf{k}\sigma})(n_{f\uparrow} - n_{f\downarrow})^2}{E_H - E_L} |L\rangle\langle L| - \text{H.c.} \right) + O(V^3). \tag{16.113}$$

Now the initial state has energy E_f while the excited state is either a state with one conduction electron and no f-electrons, with energy $\epsilon_{\mathbf{k}}$, or a state with two f-electrons and one conduction hole, with energy $2E_f + U - \epsilon_{\mathbf{k}}$, so we may write

$$S = \sum_{\mathbf{k}\sigma} \left[V_{\mathbf{k}} \frac{c^\dagger_{\mathbf{k}\sigma} f_\sigma (1 - n_{f\,-\sigma})}{\epsilon_{\mathbf{k}} - E_f} + V^*_{\mathbf{k}} \frac{f^\dagger_\sigma c_{\mathbf{k}\sigma} n_{f\,-\sigma}}{E_f + U - \epsilon_{\mathbf{k}}} - \text{H.c.} \right] + O(V^3), \tag{16.114}$$

where we have replaced $f_\sigma (n_{f\,\uparrow} - n_{f\downarrow})^2 = f_\sigma (1 - n_{f\,-\sigma})^2 = f_\sigma (1 - n_{f\,-\sigma})$ and $f^\dagger_\sigma (n_{f\,\uparrow} - n_{f\downarrow})^2 = f^\dagger_\sigma n^2_{f\,-\sigma} = f^\dagger_\sigma n_{f\,-\sigma}$. Rearranging this a little, we obtain

$$S = \sum_{\mathbf{k},\sigma} \left[V_{\mathbf{k}} \left((1 - n_{f\,-\sigma}) \frac{c^\dagger_{\mathbf{k}\sigma} f_\sigma}{\epsilon_{\mathbf{k}} - E_f} + n_{f\,-\sigma} \frac{c^\dagger_{\mathbf{k}\sigma} f_\sigma}{\epsilon_{\mathbf{k}} - (E_f + U)} \right) - \text{H.c.} \right] + O(V^3). \tag{16.115}$$

Example 16.5 Composite nature of the f-electron.

The Kondo model only involves the spin of the f-electron, and the f-creation and annihilation operators have apparently completely disappeared. To find out what has happened to them, consider adding a source term for the f-electrons,

$$H_S = \sum_\sigma (f^\dagger_\sigma \eta_\sigma + \bar{\eta}_\sigma f)_\sigma, \tag{16.116}$$

into the Anderson impurity model, so that now $H \to H[\bar{\eta}, \eta] = H + H_S$, so that the functional derivatives of the partition function

$$Z[\eta_\sigma, \eta_\sigma] = Z_0 \left\langle T \exp \left[- \int_0^\beta d\tau f^\dagger_\sigma(\tau)\eta_\sigma(\tau) + \bar{\eta}_\sigma(\tau) f_\sigma(\tau) \right] \right\rangle \tag{16.117}$$

generate correlation functions of the fermion operators:

$$\frac{\delta}{\delta \bar{\eta}_\sigma} \to f_\sigma(\tau), \qquad -\frac{\delta}{\delta \eta_\sigma} \to f^\dagger_\sigma(\tau). \tag{16.118}$$

(a) Repeat the Schrieffer–Wolff transformation for the case of constant hybridization $V_{\mathbf{k}} = V$ and particle–hole symmetry to show that the Kondo model with source terms now becomes

$$H_K[\bar{\eta}, \eta] = \sum_{\mathbf{k}\sigma} \epsilon_{\mathbf{k}} c^{\dagger}_{\mathbf{k}\sigma} c_{\sigma} + J \left(\psi^{\dagger}(0) + V^{-1}\bar{\eta}\right) \vec{\sigma} \left(\psi(0) + V^{-1}\eta\right) \cdot \vec{S}. \tag{16.119}$$

(b) By differentiating this expression with respect to $\bar{\eta}_\sigma$, show that in the Kondo model the original f-electron operator has now become a *composite operator* involving a combined conduction electron and spin-flip, as follows:

$$f_\alpha \equiv \frac{\delta H_K[\bar{\eta}, \eta]}{\delta \bar{\eta}_\alpha} = \frac{J}{V} \left(\sigma_{\alpha\beta} \cdot \vec{S}\right) \psi(0)_\beta. \tag{16.120}$$

When a Fermi liquid develops, it is this object that behaves like a resonant bound-state fermion.

Solution

(a) In the Anderson model, we can absorb the source term into the hybridization, writing it in the form

$$\mathcal{V} = \sum (V\psi^{\dagger}_{\sigma}(0) + \bar{\eta}_\sigma) f_\sigma + \text{H.c.}, \tag{16.121}$$

so that in the hybridization we have replaced $\psi_\sigma(0) \to \psi_\sigma(0) + \frac{1}{V}\eta_\sigma$. If we now repeat the Schrieffer–Wolff transformation, the spin exchange term in the Kondo model takes the form

$$H_K[\bar{\eta}, \eta] = \sum_{\mathbf{k}\sigma} \epsilon_{\mathbf{k}} c^{\dagger}_{\mathbf{k}\sigma} c_{\sigma} + J \left(\psi^{\dagger}(0) + V^{-1}\bar{\eta}\right) \vec{\sigma} \left(\psi(0) + V^{-1}\eta\right) \cdot \text{S}. \tag{16.122}$$

(b) If we now differentiate H_K with respect to $\bar{\eta}$, we obtain

$$f_\sigma \equiv \left.\frac{\delta H_K[\bar{\eta}, \eta]}{\delta \eta_\sigma}\right|_{\eta,\bar{\eta}=0} = \frac{J}{V} \left[(\vec{\sigma} \cdot \vec{S})\psi(0)\right]_\sigma. \tag{16.123}$$

16.9 "Poor man's" scaling

We now apply the scaling concept to the Kondo model. This was originally carried out by Anderson and Yuval [12–14] using a method formulated in the time rather than the energy domain. The method presented here follows Anderson's "poor man's" scaling approach [31, 32], in which the evolution of the coupling constant is followed as the bandwidth of the conduction sea is reduced. The Kondo model is written

$$H = \sum_{|\epsilon_k|<D} \epsilon_k c^{\dagger}_{k\sigma} c_{k\sigma} + H^{(I)}$$